J|A|C|S COMMUNICATIONS

Published on Web 09/01/2010

Fluorinated Diaminocyclopentanes as Chiral Sensitive NMR Probes of RNA Structure

Roba Moumné,[†,§] Morgane Pasco,[†,§] Elise Prost,[†] Thomas Lecourt,[†] Laurent Micouin,*[,†] and Carine Tisné*[,‡]

UMR8638 and UMR8015, CNRS-Paris Descartes University, Faculté de Pharmacie, 4 av. de l'Observatoire, 75006 Paris, France

Received May 10, 2010; E-mail: laurent.micouin@parisdescartes.fr; carine.tisne@parisdescartes.fr

Abstract: The supramolecular chiral recognition between *rac*-**2a** and several structured RNA leads to a distinct ^{19}F NMR signal splitting. The ^{19}F NMR analysis of the diastereomeric pairs formed upon binding of this racemic probe delivers a topological footprint of the RNA. This phenomenon can be exploited to investigate dynamic events involving structural equilibria, as demonstrated in a melting experiment. This work provides a proof of concept that small fluorinated moderate binders can act as external probes of RNA structures.

RNA molecules are major actors in numerous cellular processes and are nowadays considered as potential drug targets.[1] RNA-regulated biological processes are generally triggered by conformational interplay between several secondary and/or tertiary structures.[2] Even for short oligonucleotides, the study of these dynamic events can be complex and requires the development of structural probes.[3] One general approach for obtaining information on RNA dynamic structures is to introduce an ^{19}F nucleus into the RNA and follow conformational changes[4] or binding events[5] by ^{19}F NMR spectroscopy. This strategy has some limitations, as the fluorine atom itself can modify the physicochemical properties of the RNA[6] and simple methods for selective labeling of RNA bearing post-transcriptional modifications are still lacking.[7] An alternative strategy is to develop small molecular external probes. However, this approach also has its own limitations, as probes with good affinity can alter the interconversion of the RNA between its multiple functional states.[8]

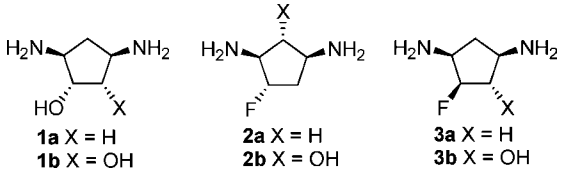

Figure 1. Fluorinated Diaminocyclopentanes.

In our ongoing work on the fragment-based design of RNA ligands, we have shown that diaminocyclopentanes **1** (Figure 1) are able to bind to different transfer RNA (tRNA), in particular $tRNA^{Lys}_3$, the primer of HIV-1 reverse transcription.[9] Here we present the use of fluorinated diaminocyclopentanes as chiral sensitive NMR probes for RNA structures. Racemic fluorinated diaminocyclopentane **2a** was prepared from alcohol **4**[10] in a straightforward manner (Scheme 1).

Scheme 1. Synthesis of Fluorodiaminocyclopentanes *rac*-**2a** and (+)-**2a**[a]

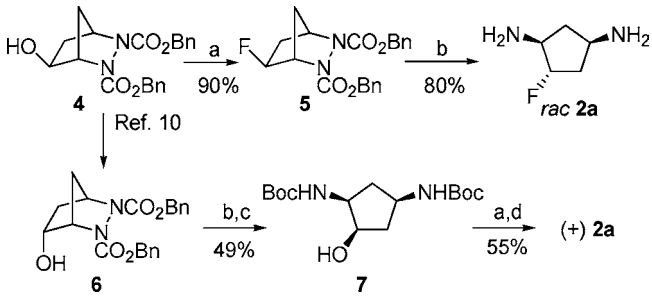

[a] Reagents and conditions: (a) DAST, DCM, 0 °C; (b) H_2, Pd/C, MeOH; (c) Boc_2O, K_2CO_3, THF/H_2O; (d) HCl, AcOEt.

Although compound **4** can be prepared in an enantiomerically enriched form by a rhodium-catalyzed desymmetrization reaction, the creation of the carbon−fluorine bond with retention of relative configuration involves a transient *meso*-aziridinium[11] and is therefore a racemizing process. Each enantiomer of **2a** was obtained separately via a different route involving the inversion of enantiomerically enriched *cis*-diaminocyclopentanol **7**.

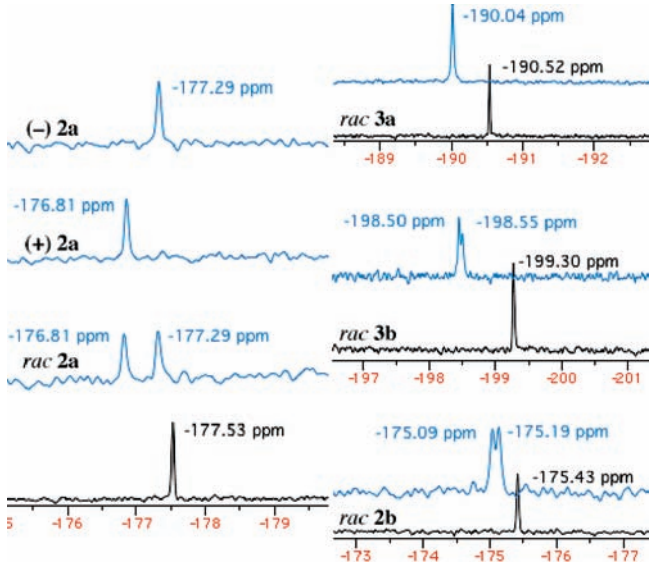

Figure 2. ^{19}F NMR spectra of fluorinated diaminocyclopentanes with $tRNA^{Lys}_3$: (black) 1 mM solution of fluorinated diaminocyclopentane in KPO_4 buffer (10 mM, pH 6.5) using 1% TFE as an internal standard at 293 K; (blue) after additions of $tRNA^{Lys}_3$ (ligand/RNA ratio = 16:1).

The interaction of **2a** (racemic or enantioenriched) with $tRNA^{Lys}_3$ was investigated by ^{19}F NMR spectroscopy (Figure 2, left). Upon

[†] UMR 8638.
[‡] UMR 8015.
[§] These authors contributed equally.

binding to $tRNA^{Lys}_3$, each enantiomer of **2a** gave rise to a resonance shift in the ^{19}F NMR signal without intensity variation, indicating that the exchange between the free and bound forms is in the fast regime on the NMR chemical shift time scale. Moreover, this resonance shift proved to be different for each enantiomer. A split of 0.5 ppm between the two signals was obtained, indicating a complete NMR resolution of the racemic sample, even though the two enantiomers bind to $tRNA^{Lys}_3$ with the same dissociation constant (~1 mM) and at the same binding site.[12]

The interaction of racemic compounds *rac*-**2b**, -**3a**, and -**3b** with $tRNA^{Lys}_3$ was then investigated under similar conditions (Figure 2, right).[13] A shift or/and NMR resolution of the fluorine resonances were also observed, and the signal splitting varied with the structure of the ligand. All of these ligands (racemic or enantioenriched) bind to $tRNA^{Lys}_3$ with K_d in the millimolar range.[12] Therefore, these differences in chemical shift variations are a direct consequence of chiral supramolecular recognition between the RNA and its bound ligand, with *rac*-**2a** being the most sensitive to this chiral molecular recognition.

The binding site of *rac*-**2a** to $tRNA^{Lys}_3$ was identified to be located in its T-arm by 2D $^1H-^{15}N$ TROSY NMR experiments.[12] Interestingly, the ^{19}F NMR spectrum of *rac*-**2a** mixed with a small RNA hairpin corresponding to the T-arm leads also to a fluorine NMR signal splitting, whereas the use of a hairpin corresponding to the D-arm does not lead to the same phenomenon (Figure 3). The signal shift and line width broadening observed with the D-arm hairpin reflect nonspecific weak interactions, since the broadening decreases with increasing ionic strength of the medium.[12] This was also confirmed by the absence of NMR chemical signal perturbation of the tRNA D-arm in the 1D ^1H NMR spectrum in the presence of *rac*-**2a**.[12] The observed splitting of the ^{19}F NMR signal thus appears as a chiral footprint of $tRNA^{Lys}_3$ T-arm structures on *rac*-**2a**.

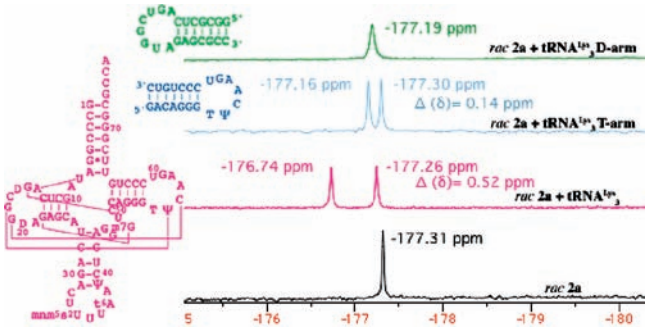

Figure 3. ^{19}F NMR spectra of (bottom to top) rac **2a** (1 mM) (black), *rac*-**2a** (1 mM) with $tRNA^{Lys}_3$ (pink), *rac*-**2a** (1 mM) with $tRNA^{Lys}_3$ T-arm (light-blue), and *rac*-**2a** (1 mM) with $tRNA^{Lys}_3$ D-arm (green) [ligand/RNA ratio = 16:1 in 10 mM KPO_4 buffer (pH 6.5) containing 50 mM KCl at 293 K]. The slight difference in the chemical shifts of *rac*-**2a** in Figure 3 and Figure 2 is a consequence of the presence of 50 mM KCl in this experiment.

The observed signal splitting increased when the RNA/*rac*-**2a** ratio was increased (Figure 4). Indeed, since the interaction occurs in the fast regime on the NMR chemical shift time scale, the averaged ^{19}F NMR signal for the free and bound states of the ligand shifts toward the bound-ligand signal as the RNA/ligand ratio increases.

The binding of *rac*-**2a** was then studied with different RNAs, all having the same cloverleaf secondary structure and similar tertiary structure: $tRNA_f^{Met}$, the *Escherichia coli* initiator tRNA; $tRNA_m^{Met}$, the *E. coli* methionine elongator tRNA; the yeast $tRNA^{Phe}$; and a small hairpin mimicking the T-arm of *E. coli* $tRNA_f^{Met}$ (Figure 5). A chiral NMR resolution leading to a distinct

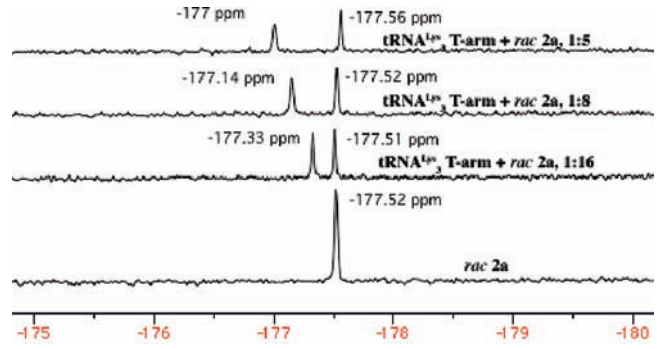

Figure 4. ^{19}F NMR spectra of *rac*-**2a** (1 mM) with increasing concentrations of $tRNA^{Lys}_3$ T-arm [in 10 mM KPO_4 buffer (pH 6.5) at 293 K].

splitting of the signal was observed for all of these RNAs, although the K_d values for *rac*-**2a** are similar.[12] These experiments show that the extreme sensitivity of the fluorine nucleus to its local chiral environment allows the analysis of RNA secondary and tertiary structures by a simple visualization of diastereomeric interactions, providing a footprint of the RNA on the ligand.

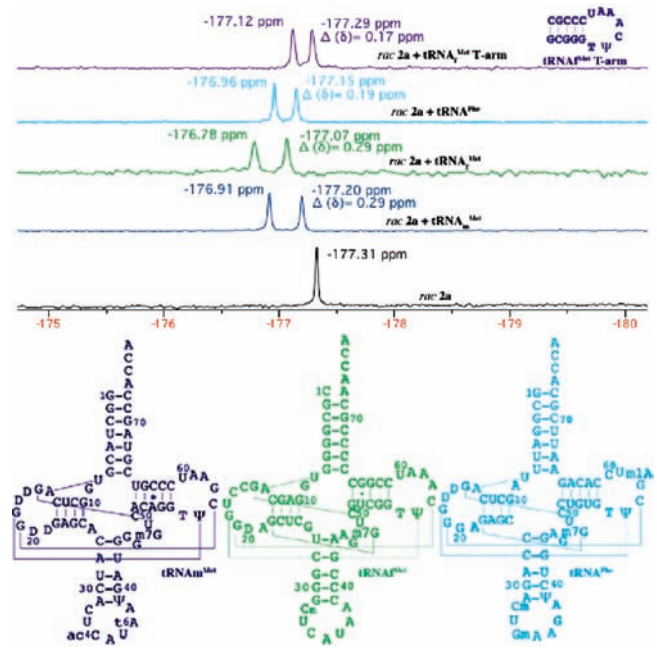

Figure 5. ^{19}F NMR spectra of *rac*-**2a** (1 mM) with different RNA (ligand/RNA ratio = 16:1) in KPO_4 buffer (10 mM, pH 6.5), 50 mM KCl, at 293 K: (dark-blue) $tRNA_m^{Met}$; (green) $tRNA_f^{Met}$; (sky-blue) $tRNA^{Phe}$; (purple) $tRNA_f^{Met}$ T-arm.

We investigated the possibility of using *rac*-**2a** as a probe to monitor dynamic structural changes of RNA by following the simplest case of a hairpin RNA thermal melting as a proof of concept (Figure 6). The study of the ^{19}F NMR shift of *rac*-**2a** in the presence of $tRNA^{Lys}_3$ T-arm hairpin showed a strong shift for each enantiomer's ^{19}F resonance upon a stepwise increase in the temperature, with a concomitant decrease of the splitting between the two signals of the diastereomeric pairs. Importantly, a complete coalescence of the two ^{19}F NMR signals was obtained at 350 K as a result of the complete unfolding of the RNA.[14] The initial splitting was again recovered after RNA refolding when the sample was cooled to the initial temperature. Thus, the conformational change that occurred during the melting of the RNA hairpin can successfully be followed using the racemic probe *rac*-**2a** (Figure 6).

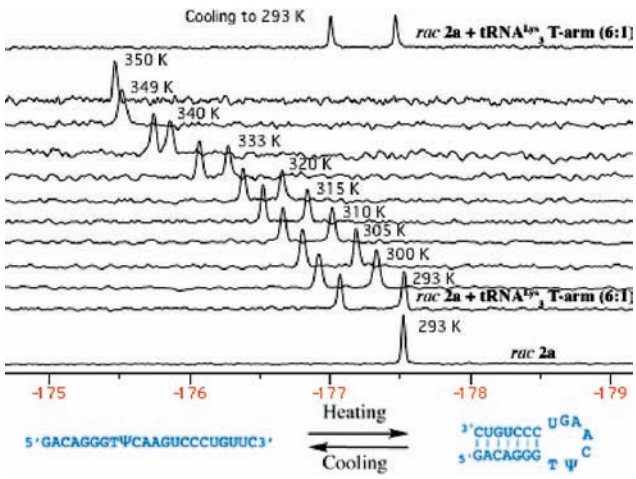

Figure 6. Melting of an RNA hairpin in the presence of *rac*-**2a** followed by ^{19}F NMR spectroscopy. ^{19}F spectra are shown for (bottom) *rac*-**2a** (1 mM); (middle) 6:1 *rac*-**2a**/RNA in KPO_4 buffer (10 mM, pH 6.5), the temperature varying from (bottom) 293 to (top) 350 K; and (top) 6:1 *rac*-**2a**/RNA after heating to 350 K and then cooling to 293 K.

In summary, ^{19}F NMR spectroscopy is very insightful because of the high sensitivity of the fluorine shielding parameters to changes in the local environment. Fluorinated diaminocyclopentanes are useful small external probes for studying RNA structures. The ^{19}F NMR analysis of the diastereomeric pairs formed upon binding of these racemic probes delivers a topological footprint of the RNA. This phenomenon can be exploited to investigate dynamic events involving structural equilibria, as demonstrated in a melting experiment. As diaminocyclopentanes are only modest binders, they bind to various RNA with K_d in the millimolar range in a fast-exchange NMR mode. This low affinity ensures that the probe itself has little influence on the static or dynamic structure of the target. This approach is user-friendly, as it does not require RNA site-specific modification, and the great NMR sensitivity of the naturally abundant ^{19}F nucleus allows its application with a widely available, routine NMR equipment.[15] The use of such fluorinated probes as reporters for the screening of small molecular RNA binders and the investigation of RNA-regulated cellular processes is under investigation in our laboratories.

Acknowledgment. Financial support from CNRS, MRT (grant to M.P.), ANRS (grant to R.M.) and ANR (Research Project PCV TriggeRNA) is acknowledged. Dr. S. Bombard is acknowledged for help in Tm determination.

Supporting Information Available: Synthesis and characterization of ligands, NMR sample preparations, K_d determinations, and NMR footprint. This material is available free of charge via the Internet at http://pubs.acs.org.

References

(1) (a) Gallego, J.; Varani, G. *Acc. Chem. Res.* **2001**, *34*, 836–843. (b) Thomas, J. R.; Hergenrother, P. J. *Chem. Rev.* **2008**, *108*, 1172–1224.
(2) (a) Schwalbe, H.; Buck, J.; Fürtig, B.; Noeske, J.; Wöhnert, J. *Angew. Chem., Int. Ed.* **2007**, *46*, 1212–1219. (b) Batey, R. T.; Rambo, R. P.; Doudna, J. A. *Angew. Chem., Int. Ed.* **1999**, *38*, 2326–2343.
(3) Liu, J.; Cao, Z.; Lu, Y. *Chem. Rev.* **2009**, *109*, 1948–1998.
(4) (a) Graber, D.; Moroder, H.; Micura, R. *J. Am. Chem. Soc.* **2008**, *130*, 17230–17231. (b) Puffer, B.; Kreutz, C.; Rieder, U.; Ebert, M.-O.; Konrat, R.; Micura, R. *Nucleic Acids Res.* **2009**, *37*, 7728–7740.
(5) Kreutz, C.; Kählig, H.; Konrat, R.; Micura, R. *Angew. Chem., Int. Ed.* **2006**, *45*, 3450–3453.
(6) Kreutz, C.; Kählig, H.; Konrat, R.; Micura, R. *J. Am. Chem. Soc.* **2005**, *127*, 11558–11559.
(7) Henning, M.; Scott, L. G.; Sperling, E.; Bermel, W.; Williamson, J. R. *J. Am. Chem. Soc.* **2007**, *129*, 14911–14921.
(8) This dynamic equilibrium shift occurs, for instance, upon binding of aminoglycosides to 16S RNA, leading eventually to their antibiotic activity.
(9) (a) Chung, F.; Tisné, C.; Lecourt, T.; Seijo, B.; Dardel, F.; Micouin, L. *Chem.—Eur. J.* **2009**, *15*, 7109–7116. (b) Chung, F.; Tisné, C.; Lecourt, T.; Dardel, F.; Micouin, L. *Angew. Chem., Int. Ed.* **2007**, *46*, 4489–4491.
(10) Pérez Luna, A.; Ceschi, M.-A.; Bonin, M.; Micouin, L.; Husson, H.-P.; Gougeon, S.; Estenne-Bouhtou, G.; Marabout, B.; Sevrin, M.; George, P. *J. Org. Chem.* **2002**, *67*, 3522–3524.
(11) Bournaud, C.; Bonin, M.; Micouin, L. *Org. Lett.* **2006**, *8*, 3041–3043.
(12) See the Supporting Information.
(13) The characterization of compounds **2b**, **3a**, and **3b** is described in the Supporting Information, and the synthesis of these compounds will be described elsewhere.
(14) The complete unfolding of the hairpin structure at 350 K was verified by the UV melting curve of the hairpin in the presence of the ligand (see the Supporting Information).
(15) All of the ^{19}F NMR experiments were conducted on a 300 MHz (H value) NMR spectrometer with a standard QNP probe.

JA1037885